Obrabotka metallov -
Metal Working and Material Science

Journal homepage: http://journals.nstu.ru/obrabotka_metallov

Dimensional analysis and ANN simulation of chip-tool interface temperature during turning SS304

*Atul Kulkarni [1, a], Satish Chinchanikar [1, b, *], Vikas Sargade [2, c]*

[1] Vishwakarma Institute of Information Technology, Survey No. 3/4, Kondhwa (Budruk), Pune - 411048, Maharashtra, India
[2] Dr. Babasaheb Ambedkar Technological University, Vidyavihar, Lonere, Dist. Raigad - 402103, Maharashtra, India

[a] https://orcid.org/0000-0002-6452-6349, ✉ atul.kulkarni@viit.ac.in, [b] https://orcid.org/0000-0002-4175-3098, ✉ satish.chinchanikar@viit.ac.in,
[c] https://orcid.org/0000-0001-8855-112X, ✉ vgsargade@dbatu.ac.in

ARTICLE INFO

ABSTRACT

Introduction. During machining, the resulting temperature has a wider and more critical impact on machining performance. During machining, the power consumption is mainly converted into heat near the cutting edge of the tool. Almost all the work performed during plastic deformation turns into heat. Researchers have put a lot of effort into measuring the cutting temperature during machining, as it significantly affects tool life and overall machining performance. **The purpose of the work:** to investigate the temperature of the chip-tool interface, taking into account the influence of cutting parameters and the type of tool coating during *SS304* turning. The chip-tool interface temperature is measured by changing the cutting speed and feed with a constant cutting depth for uncoated and *PVD* single-layer *TiAlN* and multi-layer *TiN/TiAlN* coated carbide tools. In addition, an attempt is made to develop a model for predicting the temperature of the chip-tool interface using dimensional analysis and *ANN* simulating to better understand the process. **The methods of investigation.** Experiments are carried out with varying the cutting speed (140-260 m/min), feed (0.08-0.2 mm/rev) and a constant cutting depth of 1 mm. The chip-tool interface temperature is measured using the tool-work thermocouple principle. The Calibration Setup is designed to establish the relationship between the produced electromotive force (*EMF*) and the cutting temperature during machining. Statistical dimensional analysis and artificial neural network models have been developed to predict the temperature of the chip-tool interface. Tangential cutting force and chip attributes such as chip width and thickness are also measured depending on the cutting conditions, which is a prerequisite for dimensional analysis simulation. **Results and Discussion.** A tool made of *TiAlN* carbide with *PVD* coating had a lower temperature at the chip-tool interface than a tool with *TiN/TiAlN* coating. It has been observed that the chip-tool interface temperature increases prominently with the cutting speed, followed by the chip cross-sectional area and the specific cutting pressure. However, a lower cutting force was observed when using a carbide tool with a multi-layer *TiN/TiAlN* coating, which can be attributed to a lower coefficient of friction created by the front surface of this tool for flowing chips. On the other hand, the greatest cutting force was observed in uncoated carbide tools. It was noticed that the developed models allow predicting the temperature of the chip-tool interface with an absolute error of 5%. However, the lowest average absolute error of 0.78% was observed with the *ANN* model and, therefore, can be reliably used to predict the chip-tool interface temperature during *SS304* turning.

Introduction

Austenitic stainless steel, the most consumed nonmagnetic steel, is categorized under difficult-to-cut materials. This is due to its tendency to produce long, sticky, and stringy chips along with the formation of the built-up edge during machining that produces less tool life and poor surface finish. The selection of

---

* Corresponding author
Chinchanikar Satish, Ph.D. (Engineering), Professor
Vishwakarma Institute of Information Technology,
Pune, Maharashtra, India
Tel.: 91-2026950441, **e-mail:** satish.chinchanikar@viit.ac.in

cutting tool material, its geometry, and cutting conditions play an important role while machining these steels.

The researchers observed higher chip-tool interface temperature with uncoated tools followed by *TiC/TiN* and *TiC/Al₂O₃/TiN* coated carbide tools. The interface temperature was observed increasing rapidly with the increase in the feed and cutting speed. However, the increase in the cutting temperature accelerated the tool wear and significantly affected the tool life [1-2]. Pal *et al.* [3] developed mathematical model to predict the chip-tool interface temperature. Their study showed that the cutting speed and cutting depth were more significant for increasing the temperature of the interface. Abhang *et al.* [4] developed the thermoelectric relationship between the cutting tool and the work material. Their study showed that the cutting speed followed by feed had a prominent effect on cutting temperature during turning of *EN-31* steel.

Alvelid [5] used the tool-work thermocouple principle. The author carried out the calibration by using the direct heating of the calibration material with the help of an electric current through a resistance element or induction coil which was placed against the contact point of the two materials. His study showed that the thermo-electric potential was significantly affected with the heating and cooling rates. Chinchanikar and Choudhury [6] also developed a mathematical model to predict the average chip-tool interface temperature based on experimental observations. Their study correlated the *EMF* (electromotive force) and the interface temperature based on the tool-work thermocouple principle. Their study showed that the cutting speed with subsequent feed has a significant impact on the interface temperature, and the cutting depth has a negligible effect on the interface temperature. In another study [7], they found higher interface temperature for harder working material than softer working material.

Panneerselvam *et al.* [8] investigated the chip-tool interface temperature for the powder metallurgy-made cutting tools. Their study revealed that cutting speed has a significant impact on the interface temperature. Bapat *et al.* [9] developed a numerical model to obtain temperature distribution in hard turning of *AISI 52100* steel. The temperature distribution model as a function of heat generation was developed using explicit *ABAQUS* and the approach of an *Arbitrary Lagrangian-Eulerian formulation (ALE)*. Their study showed that cutting temperature increases with the increase in cutting speed. The simulated results of the temperature distribution showed a good agreement with the results available in the literature.

Dhar *et al.* [10] reported rapid deterioration in the surface roughness due to the increase in cutting temperature and stress at the tool tip. The tool-work thermocouple principle was used to measure the chip-tool interface temperature. Anagonye *et al.* [11] performed the calibration of the tool and work materials with the oxy-acetylene torch that was used as a heating source for the tool-work thermocouple technique. Their study showed decrease in the cutting temperature with the increase in the included angle and nose radius of the insert due to availability of more area for conduction of heat.

It follows from the analyzed literature that the cutting parameters, especially the cutting speed and feed, significantly affect the temperature of the chip-tool interface. Most of the studies attempted measurement of cutting temperature during machining using the tool-work thermocouple method. However, there is very little research on the cutting temperature, considering the influence of cutting parameters and the type of tool coating when turning *SS304*. Moreover, very few attempts are found on modeling cutting temperature using dimensional analysis and artificial neural networks. Considering the above facts, the present work investigates the chip-tool interface temperature during turning *SS304* with uncoated and *PVD* single-layer *TiAlN* and multi-layer *TiN/TiAlN* coated carbide tools. In addition, for a better understanding of the process, an attempt was made to develop a model for predicting the temperature of the chip-tool interface using size analysis and ANN simulation.

Experimental Details

In the present work, the chip-tool interface temperature was investigated during turning of *SS304* stainless steel workpiece having the diameter and length of 90 mm and 300 mm, respectively, using uncoated and *PVD* single-layer *TiAlN* and multi-layer *TiN/TiAlN* coated carbide tools. The *ISO* specifications of the uncoated insert and tool holder used in the present study are given in Table 1. The nose radius of the

Table 1

The ISO specifications of cutting insert and tool holder

Particulars	Details
ISO designation of cutting insert	CNMG120408 (MG-MS)
Including angle	80°
Rake angle	–6°
Clearance angle	5°
Approach angle	95°
ISO designation of tool holder	PCLNL2525M12

selected cutting insert was 0.8 mm, and the edge radius of the insert was approximately 20 µm. Turning experiments were performed on the *CNC* lathe. The chip-tool interface temperature was investigated under dry turning at cutting speeds of 140, 200, and 240 m/min, feed of 0.08, 0.14, 0.2, and 0.26 mm/rev, and a constant depth of cut 1 mm. The cutting parameters were decided based on a literature review, machine capability, and recommendations of the cutting tool manufacturer.

In machining, the temperature generated has a wider and critical impact on machining performance. During machining, the power consumption is mainly converted into heat near the cutting edge of the tool. Almost all the work performed during plastic deformation turns into heat. In the present study, the law of the thermoelectricity (*Seebeck effect*) principle was used to correlate the difference in temperature between the hot junction and the cold junction of two dissimilar materials with the generated electromotive force (*EMF*). However, the presence of third material would be undesirable as it can alter the final output due to the formation of parasitic *EMF* at the second junction. As it alters the final output, precautionary measures are required to be taken to eliminate it. Therefore, insulation of the work/tool material plays important role in getting accurate results from the tool-work thermocouple method.

Initially, the workpiece was clamped with the help of chuck and supported by using the tailstock center while machining. Therefore, care was taken to isolate the workpiece from the jaws of the chuck. The workpiece was insulated by using a special type of Teflon tape and bush as shown in Fig. 1. Also, the chuck jaw pressure was adjusted and kept as optimum to prevent penetration of the jaws across the insulation. After insulating the workpiece from one end i.e., from the chuck, insulation of the workpiece from the
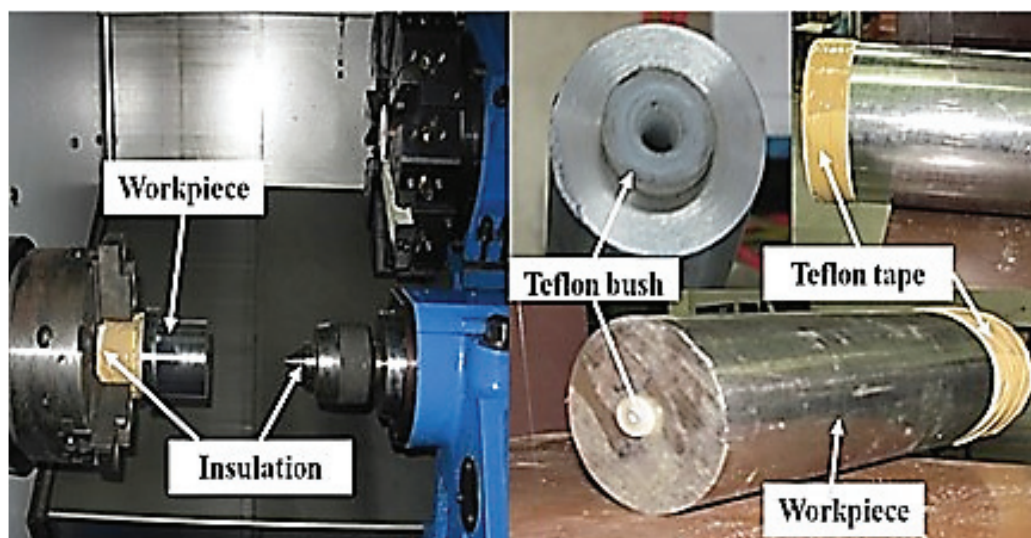

Fig. 1. Insulation of the workpiece with the inserted plugs

tailstock was necessary to completely isolate the workpiece from the machine body. In this regard, the revolving center was coated with epoxy gel-coating material and Teflon insulating plugs (non-conductive material plugs) were used. As the tool holder is in direct contact with the turret and ultimately with the machine body, the different parts of the tool holder that come directly in contact with the cutting tool were coated. The coating material used for the coating of the tool holder (a shim, L-shape lever, packing, and shank body) was epoxy-polyester with a coating thickness of around 20 μm.

Tool and workpiece junction at the time of machining was considered as hot junction while the carbon brush touching the workpiece was cold junction as shown in Fig. 2. The connection leads from the tool were taken through the small opening provided on the tool holder shank. A carbon brush was used to make wiring connections from the rotating workpiece. A special stand and spring-loaded holder were designed and fabricated to maintain a uniform and firm contact between the carbon brush and the workpiece as shown in Fig. 2.
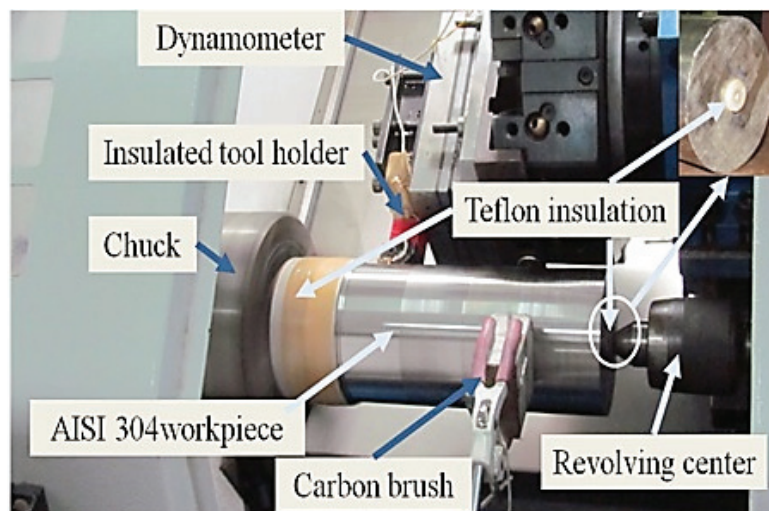

Fig. 2. Tool-work thermocouple machining setup

One end of copper wire was placed between the insert and tool holder and the other end was connected to the voltmeter. One additional copper wire was used for completing the electric circuit. One end of the wire was attached to the carbon brush and the other end to the voltmeter. Copper wire of 1 mm diameter was used for the connection purpose and its length was maintained constant during experiments and calibration.

Calibration Setup was developed to establish the relationship between the *EMF* produced and cutting temperature during machining. Tool-work thermocouple junction was constructed using a long continuous chip and tungsten carbide insert. An electric air heater was used as a heating element for the work-tool junction. It simulated the thermal phenomena in machining. It is reported in the literature that the calibration temperature should be more than half the melting point of the working material (*SS304* melting point: 1,453 °C) [1, 2]. Hence, an electric air heater made of Inconel material having a capacity of 2 KW was selected and it can generate 1,000 °C temperature at red-hot conditions. A standard alumel-chromel thermocouple wire was mounted at the junction of the workpiece and insert.

For calibration of the chip-tool interface temperature, initially, the workpiece and tool materials to be calibrated were clamped to ensure the proper contact between it. Then, one end of the copper wire was connected to the tool and workpiece and another end was connected to the voltmeter terminals. The electric air heater was then brought into contact with the junction point to heat the junction point. A standard K-type (chromel-alumel) thermocouple was held at the work-tool junction and connected to the temperature indicator. The whole assembly was kept in a container that was insulated with glass wool to reduce heat losses. The electric heater was turned on and the junction point was heated gradually up to 1,000 ^{o}C,
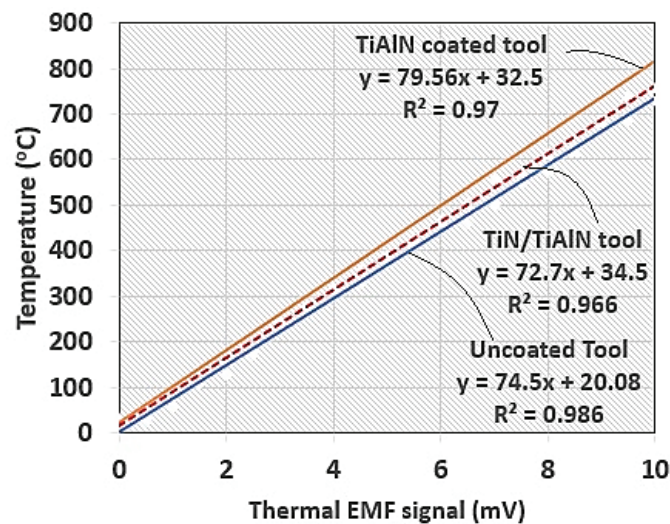
Fig. 3. Calibration curves for uncoated and *PVD*
single-layer *TiAlN* and multi-layer *TiN/TiAlN* coated
carbide tools

and corresponding *EMF* was recorded. The calibration graph for the combination of uncoated and *PVD* single-layer *TiAlN* and multi-layer *TiN/TiAlN* coated carbide tools for *SS304* work material is shown in Fig. 3.

Results and Discussion

Significant research around the world is aimed at improving the workability of *SS304*. Table 2 shows the experimental results of cutting temperatures measured during dry turning of *SS304* steel with uncoated and *PVD* single-layer *TiAlN* and multi-layer *TiN/TiAlN* coated carbide tools at different cutting conditions. Fig. 4 illustrates the influence of the cutting speed and feed on the cutting temperature when using uncoated and *PVD* single-layer *TiAlN* and multi-layer *TiN/TiAlN* coated carbide tools.

In recent years, researchers have been paying considerable attention to the development of predictive models to measure performance during machining. In the present work, statistical-based, dimensional analysis, and artificial neural network models are developed to predict the chip-tool interface temperature.

Table 2

Cutting temperature for different tools varying with cutting conditions

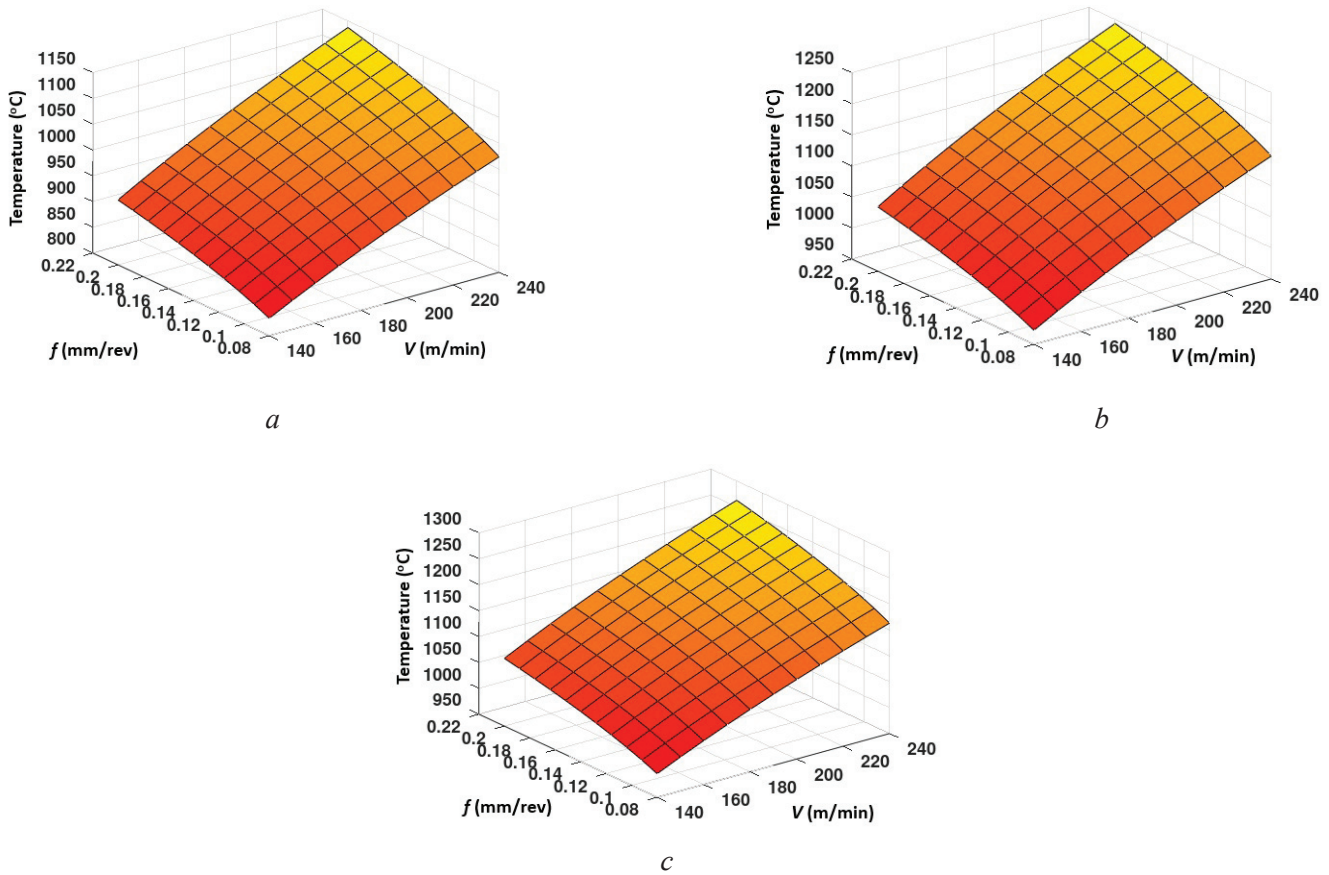| Expt. no.	Cutting speed (m/min)	Feed (mm/rev)	Chip-tool interface temperature		
			Uncoated	*TiAlN* coated	*TiN/TiAlN* coated
1	140	0.08	825	930	996
2	140	0.14	900	1,039	1,047
3	140	0.2	939	1,041	1,081
4	200	0.08	933	1,109	1,104
5	200	0.14	1,029	1,169	1,161
6	200	0.2	1,039	1,200	1,199
7	260	0.08	1,078	1,186	1,191
8	260	0.14	1,120	1,204	1,252
9	260	0.2	1,175	1,257	1,293

Fig. 4. Cutting temperature for (*a*) Uncoated, (*b*) *TiAlN* coated, (*c*) *TiN/TiAlN* coated tool

The surface plots are drawn for a better understanding of the effect of process parameters on the cutting temperature. The values of the coefficients involved in the statistical-based models for different tools were calculated by regression method using the *Data-fit software*. The *R*-squared values for all the developed statistical-based models above 0.9 (Table 3) shows that developed models could be reliably used to predict the chip-tool interface temperature during the turning of *SS304* for the given combination of tool and workpiece pair.

In order to have a clear idea of the effect of the input parameters on the cutting temperature, three-dimensional (3-D) surface plots are constructed by changing the process parameters for uncoated and *PVD*-coated tools. The plots are constructed using developed empirical equations. Fig. 4 depicts the 3-D surface plots of cutting temperature during turning of *SS304* for different tools plotted using Eqs. (1) to (3).

It can be seen from Fig. 4, a–c that the cutting temperature increases with increasing cutting speed and feed. An increase in the cutting temperature can be seen as more prominent with the cutting speed followed by the feed. However, this effect can be seen as more significant with the uncoated carbide tool followed by *TiAlN* coated carbide tool. This can be also confirmed from the higher positive exponent value for the cutting speed followed by a feed from Eqs. (1) to (3).

Table 3

Statistical-based models to predict cutting temperature

Type of tool	Statistical-based models	R-squared	Eq. no.
Uncoated carbide	$T = 169.0517 V^{0.3814} f^{0.01144}$	0.98	(1)
PVD-coated *TiAlN* carbide tool	$T = 265.5113 V^{0.3074} f^{0.0874}$	0.93	(2)
PVD-coated *TiN/TiAlN* carbide tool	$T = 299.4988 V^{0.2889} f^{0.0897}$	0.99	(3)

The lowest cutting temperature observed for the uncoated carbide tool shows that the maximum heat was penetrated in the cutting tool from the rake surface. However, the higher interface temperature observed with coated tools shows that the coatings contributed to less heat penetration into the base of the tool. On the other hand, amongst the coated tools, the lowest chip-tool interface temperature was observed with the *PVD*-coated *TiAlN* carbide tool than the *TiN/TiAlN* coated tool. This can be also confirmed from the higher thermal conductivity value for the uncoated carbide tool followed by the *TiAlN* coating and *TiN/TiAlN* coating. Thermal conductivity of uncoated tool, *PVD*-coated *TiAlN* and *TiN/TiAlN* coated tools are 80 W/m-K, 6.7 W/m-K, and 5.1 W/m-K, respectively [12–14]. The thermal conductivity of the uncoated carbide tool is more compared to the *TiAlN* and *TiN/TiAlN* coated tools. Despite the fact that the thermal conductivity increases with temperature, at high temperatures the thermal conductivity of the coated tool remains lower than that of the uncoated tool [12]. Therefore, the heat conducted in the tool during machining with the uncoated carbide tool is more compared to that of the *TiAlN* and *TiN/TiAlN* coated tools. Hence, the temperature for the uncoated carbide tool is less than that of the coated tools. These results are matching well with those reported by Grzesik [4, 13, 15].

The increase in cutting temperature prominently with the cutting speed could be attributed to an increase in the specific cutting energy. The specific cutting energy can be partitioned into two main components shear energy and frictional energy. Shear energy and frictional energy are directly proportional to the shear velocity and chip velocity respectively [16]. Therefore, an increase in the cutting speed reflects directly into the increase in the energy and hence the cutting temperature. In addition, it has been observed that the coating structure greatly affects the cutting temperature. Moreover, it has been noted that uncoated tools wear out quickly compared to coated tools, which increase the chip contact area with the tool, which leads to greater heat conduction to the tool area. While in the case of coated tools, the higher wear resistance of the coatings limits the wear and, consequently, the chip contact area with the tool and allows more heat to be removed with the current chips. The higher thermal conductivity of uncoated tools decreases its hot hardness, which results in earlier failure of the tools [17].

The problems of temperature measurement have led to the research interest in the development of mathematical models for predicting temperature during machining. Sufficient studies attempted to predict the cutting temperature using statistical-based models. The mathematical models developed by Boothroyd, Shaw, and Rapier have been also extensively used by researchers to predict the cutting temperature. In this section, simulation using dimensional analysis and artificial neural network to predict a chip-tool interface temperature with uncoated and *PVD* single-layer *TiAlN* and multi-layer *TiN/TiAlN* coated carbide tools are discussed.

Dimensional analysis of cutting temperature

In dimensional analysis, all independent variables of the problem are written down in the form of its dimensionless combinations. These independent dimensionless variables can be determined based on prior knowledge, reasoning, or experiments. The values of constants are obtained from experimental data [18-19]. In the present work, dimensional analysis is done to develop a mathematical model for obtaining the cutting temperature during the turning of *SS304* steel using uncoated and *TiAlN* coated tools. These relations are developed based on the experimental data. The physical quantities selected for the dimensional analysis are given in Table 4.

Physical quantities are expressed in such fundamental units as Mass (M), Length (L), Time (T), and Celsius temperature (D). This is the important step in which the most influencing variables that affect the cutting temperature should be selected. It was assumed that about 80…85 % of the heat is dissipated together with the chips, and, therefore, the thermal conductivity of the tool is not included in present analysis. The variables selected for the analysis are given below in Table 4. The number of fundamental quantities is four and the number of physical quantities selected in the present study is six. According to Buckingham Pi Theorem, the number of dimensionless groups required to correlate all these quantities would be equal to the difference between the number of physical quantities and the fundamental quantities which is two in the present study.

T a b l e 4

Physical quantities along with dimensional formula

Physical quantity	Symbol	Dimensional formula
Temperature (degree Celsius)	Θ	D
Cutting speed (m/min)	V_c	LT^{-1}
Chip cross-sectional area (m^2)	A_0	L^2
Specific cutting pressure (N/m^2)	S_p	$ML^{-1}T^{-2}$
Thermal conductivity of work material (W/m-K)	k	MLT^3D^{-1}
Volumetric specific heat of work material (a product of density (ρ) and specific heat of work material (C)) ([kg/m^3][J/kg-K])	ρC	$ML^{-1}T^{-2}D^{-1}$

Then four basic variables out of six physical quantities are selected in such a way that it does not make any dimensionless group in themselves. Those variables are V_c, S_p, k, and ρC. One non-basic quantity is grouped with all the four basic variables to give one dimensionless number. Let Q_1 and Q_2 are the two dimensionless groups, which are expressed as follows:

$$Q_1 = \left((V_c)^a (S_p)^b k^c (\rho C)^d\right)\theta, \tag{4}$$

$$Q_2 = \left((V_c)^e (S_p)^f k^g (\rho C)^h\right)A_0. \tag{5}$$

We write these Eqs. (4) and (5) in terms of fundamental measurements as,

$$Q_1 = (L^a T^{-a})(M^b L^{-b} T^{-2b})(M^c L^c T^{3c} D^{-c})(M^d L^{-d} T^{-2d} D^{-d})D, \tag{6}$$

$$Q_2 = (L^e T^{-e})(M^f L^{-f} T^{-2f})(M^g L^g T^{3g} D^{-g})(M^h L^{-d-h} T^{-2h} D^{-h})L^2. \tag{7}$$

After the rearranging and since Q_1 and Q_2 are dimensionless quantities, the index for each term should be zero. Therefore, equating index for each term to zero and solving equations simultaneously, we get, $a = 0$, $b = -1$, $c = 0$, $d = 1$, $e = 2$, $f = 0$, $g = -2$, and $h = 2$. Substituting these values of constant in Eqs. (6) and (7), we get,

$$Q_1 = (\rho C\theta / S_p), \tag{8}$$

$$Q_2 = \left(V_c^2 (\rho C)^2 A_o\right) / k^2. \tag{9}$$

Let expressing chip-tool interface temperature as a function of the two dimensionless groups Q_1 and Q_2 that includes dependent variable 'θ'. Cutting temperature equation using dimensional analysis (Eq. (8) and (9)) can be expressed as shown in Eq. (10).

$$\theta = C_0 (S_p / \rho C)^m \left(\left(V_c^2 (\rho C)^2 A_0\right) / k^2\right)^n, \tag{10}$$

where C_0, m, and n are constants, and its values are determined based on the experimental results. Eq. (10) can be used for determining the cutting temperature during the turning of *SS304* steel using uncoated and coated inserts. The values of the constants in Eq. (10) are obtained using experimental results of cutting temperature (Table 2) and by knowing the cutting force, chip thickness, and chip width for the given cutting conditions (Table 5).

Table 5

The cutting force, chip thickness, and chip width at cutting conditions stated in Table 2

Expt. no.	Uncoated tool			TiAlN coated tool			TiN/TiAlN coated tool		
	F_c (N)	a_c (mm)	a_w (mm)	F_c (N)	a_c (mm)	a_w (mm)	F_c (N)	a_c (mm)	a_w (mm)
1	410	0.287	1.64	354	0.3	1.5	329	0.24	1.47
2	630	0.370	1.86	536	0.32	1.8	460	0.3	1.73
3	702	0.480	1.9	610	0.35	1.83	570	0.37	1.77
4	387	0.260	1.72	318	0.28	1.663	321	0.22	1.59
5	554	0.360	1.87	498	0.3	1.76	448	0.28	1.72
6	636	0.473	1.92	582	0.33	1.83	555	0.35	1.78
7	365	0.200	1.87	366	0.27	1.646	315	0.19	1.66
8	501	0.330	1.86	512	0.29	1.733	440	0.26	1.7
9	630	0.467	1.92	556	0.315	1.84	545	0.34	1.78

The volumetric specific heat of work material (ρ_c) and the thermal conductivity (k) of work material (at 500 ^{o}C) are referred to from the literature and considered as 502 J/kg-K and 21.5 W/m-K. A_0 is the cross-sectional area of the chip and is obtained by taking the product of the chip thickness (a_c) and the chip width (a_w) for the given cutting conditions. The specific cutting pressure (S_p) is obtained by dividing the cutting force (F_c) with the product of a feed and depth of cut. The tangential cutting force (F_c) was measured by a *Kister-9257B* type cutting force dynamometer and average chip width and chip thickness were measured using a digital micrometer. The values for the constants obtained are C_0 = 1.24, m = 0.154, and n = 0.226 for uncoated carbide tool and C_0 = 1.97 and 6.63, m = 0.083 and 0.0432, n = 0.169 and 0.1605 for *TiAlN* and *TiN/TiAlN* coated carbide tools, respectively. Substituting these values in Eq. (10), the final equations to predict cutting temperature with uncoated, *TiAlN* coated and *TiN/TiAlN* coated carbide tools are given as Eqs. (11), (12), and (13), respectively.

For uncoated carbide tool,

$$\theta = 28,5636\, S_p^{0,154} V^{0,452} A_0^{0,226};\tag{11}$$

For *TiAlN* coated carbide tool,

$$\theta = 416,5528\, S_p^{-0,083} V^{0,338} A_0^{0,169};\tag{12}$$

For *TiN/TiAlN* coated carbide tool,

$$\theta = 167,9887\, S_p^{0,0432} V^{0,321} A_0^{0,1605}.\tag{13}$$

From the indicators S_p, V and of developed Eqs. (11)–(13) it can be seen that the chip-tool interface temperature depends more on the cutting speed, followed by the chip cross-sectional area and the specific cutting pressure. However, these parameters can be seen as more prominently affecting the cutting temperature for uncoated carbide tool followed by single-layer *TiAlN* coated carbide tool and multi-layer *TiN/TiAlN* coated carbide tool. The chip-tool interface temperature for uncoated carbide, single-layer *TiAlN* coated and multi-layer *TiN/TiAlN* coated carbide tools at different cutting conditions is calculated using Eqs. (11)–(13), respectively, and is shown in Table 6.
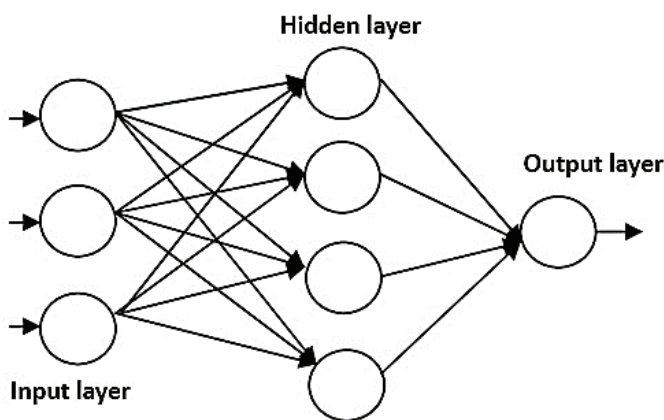
T a b l e 6

The chip-tool interface temperature with different models and tools

Expt. no.	Uncoated tool			*TiAlN* coated tool			*TiN/TiAlN* coated tool		
	SM	DA	ANN	SM	DA	ANN	SM	DA	ANN
1	834	838	837	973	963	941	996	996	987
2	889	895	936	1,021	1,017	1,027	1,047	1,049	1,045
3	926	918	942	1,054	1,055	1,041	1,081	1,082	1,049
4	955	965	939	1,085	1,103	1,099	1,104	1,114	1,098
5	1,019	1,026	1,037	1,140	1,137	1,169	1,161	1,161	1,172
6	1,061	1,061	1,038	1,176	1,183	1,217	1,199	1,203	1,195
7	1,056	1,034	1,078	1,176	1,182	1,188	1,191	1,191	1,195
8	1,126	1,114	1,119	1,235	1,229	1,210	1,252	1,245	1,254
9	1,173	1,189	1,178	1,275	1,288	1,261	1,293	1,301	1,275

Artificial neural network

Artificial neural network (*ANN*) is a computational technique that can model relationships between input and output parameters. There are different types of *ANN*, however, the most used is the multilayer perceptron (*MLP*). A typical *MLP* architecture is shown in Fig. 5. *MLP* is characterized by three different layers, namely the input layer, the hidden layer, and the output layer, which consist of an interconnected group of artificial neurons. Each neuron in a layer is connected to all the neurons in adjacent layers. The number of neurons present in the input layer and output layer is equal to the number of input variables and corresponding output values. The number of hidden layers and the neurons in those layers is user-defined.

Fig. 5. Typical *ANN* architecture

To predict output with higher accuracy, training or learning of the developed network is essential. The procedure used to perform the learning process is called a learning algorithm, the function of which is to modify the synaptic weights of the network in an orderly fashion to attain the desired output. There are various algorithms to train a neural network. One of the most preferred training algorithms is the error backpropagation algorithm. For a typical *ANN* algorithm, let $x_1, x_2, \ldots x_3$ be an input data, $y_1, y_2, \ldots y_n$ be the desired output, and $o_1, o_2 \ldots o_k$ be the output obtained from the output layer of the network when $x_1, x_2, \ldots x_3$ is presented at the input layer. At the first step, the weights and thresholds are initialized. Then, the output of each neuron $f(wi)$ is calculated from the input data and initialized weights which lead to the final output prediction of the network. Then, the error at i^{th} output node $(o_i - y_i)$ is calculated. Further, the weights between the hidden layer and output layer are modified based on an error at each output node. And weights in the previous layers are modified by back-propagating errors calculated at output layer nodes [20]. This process is repeated for a set of input and output of training data. The training stops when the output of the neural network is sufficiently close to the desired output for each set.

ANN model is developed to predict the chip-tool interface temperature considering the input parameters as the tool type, cutting speed, and feed using *MATLAB Toolbox*. The *ANN* architecture has three layers

namely input, output, and hidden layers as shown in Fig. 6. The input layer has 3 neurons, the output layer has 1 neuron, and the hidden layer has 8 neurons. A feed-forward neural network displays a data set of numeric inputs with a set of numeric targets. The *Neural Fitting app* of *MATLAB Toolbox* will help in the selection of data and for the creation and training a network and evaluate its performance using mean square error and regression analysis. A two-layer feed-forward network with sigmoid hidden neurons and linear output neurons is selected in the present study that fit multi-dimensional problems arbitrarily well, given consistent data and enough neurons in its hidden layer. The network has been trained with the Levenberg-Marquardt backpropagation algorithm.
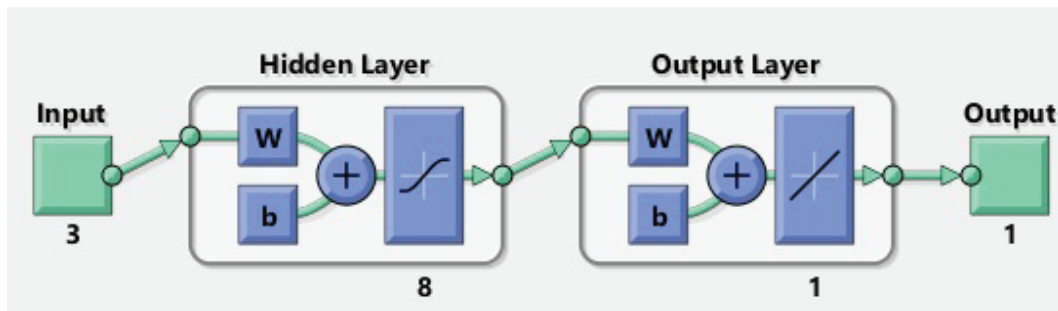

Fig. 6. ANN architecture to predict chip-tool interface temperature

In a neural network, three kinds of samples are used for the training and validation of test data. In the present work, around 70 % of the data (experimental results of cutting tool temperature) is used for training the neural network. The network is adjusted according to its error. Around 15 % of the data is used for validation of the results predicted by the trained neural network. These validation data sets are used to measure network generalization, and to halt training when generalization stops improving. And around 15 % of data is used for testing the results predicted by the neural network. These data sets do not influence on training and so provide an independent measure of network performance during and after training.

The next important step is to determine network architecture, i.e., to set the number of neurons in the fitting network hidden layer. The neurons in the hidden layer are selected by checking the accuracy of the network. The number of neurons on the hidden layer can be changed if the network does not perform well after training. In the present study, the neural network is modeled considering a different number of hidden neurons to obtain better accuracy of the predicted results. In the present study, a better-predicted accuracy of 0.995 has been observed with 8 neurons at the hidden layer. Further, the network is to be trained using either the Levenberg-Marquardt algorithm or Bayesian Regularization, or Scaled Conjugate Gradient algorithm. The Bayesian Regularization algorithm is preferred for small and noisy data sets. This algorithm results in good generalization but requires more time. Scaled Conjugate Gradient algorithm requires less memory and stops automatically when generalization stops improving. However, the researchers have mostly used the Levenberg-Marquardt algorithm for training the neural network. This algorithm is comparatively faster than other algorithms. However, this algorithm requires more memory and training automatically stops when generalization stops improving, as indicated by an increase in the mean square error of the validation samples.

Neural network training performance is measured in terms of mean squared error which is the average squared difference between outputs and targets. Lower values are more preferable and in the present work, the best validation performance of 417.9654 was observed at epoch 7. Regression (*R*) values measure the correlation between outputs (predicted values) and targets (inputs). Neural network regression graphs with regression coefficients obtained while training the model, during validation, testing, and for the entire data set are shown in Fig. 7, *a–d* respectively.

The values of regression coefficients close to 1 for training, validation, testing, and for the entire data set shows that the developed neural network model could be reliably used for predicting chip-tool interface temperature during turning of *SS304* for the given tool-workpiece pair. The results predicted by the neural network are shown in Table 6.
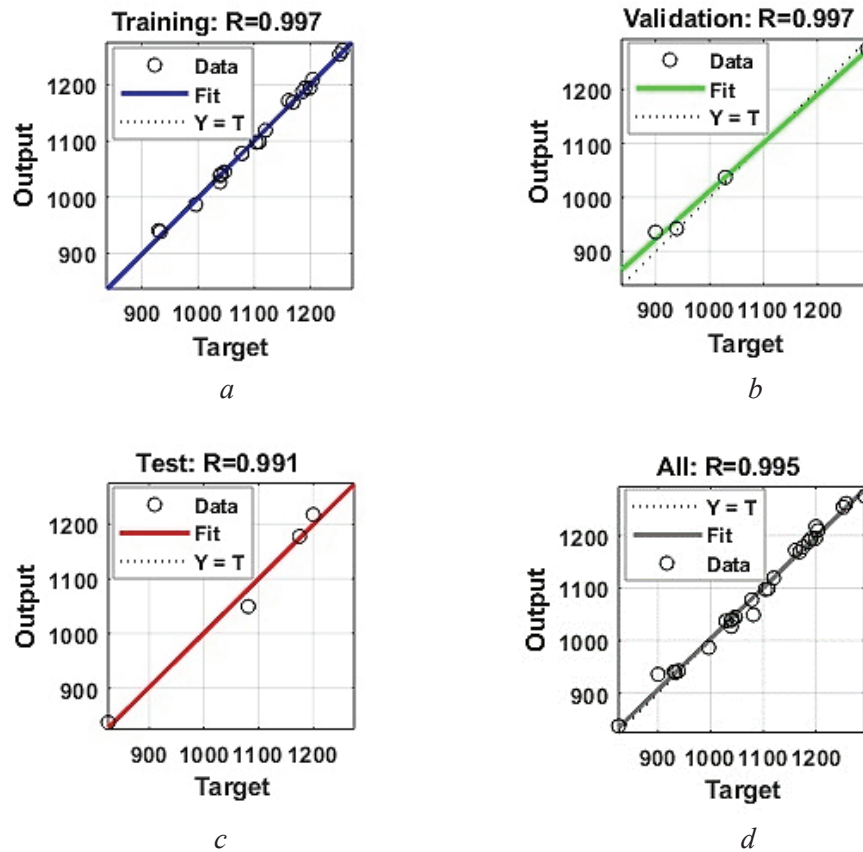
Fig. 7. Neural network:
a – Training; *b* – Validation; *c* – Test; *d* – All data set

A comparative evaluation

A comparative evaluation of the accuracy of the predicted results of chip-tool interface temperature with the statistical-based model (*SM*), dimensional analysis approach (*DA*), and artificial neural network (*ANN*) is presented in this section. The accuracy of the different models is assessed by obtaining % error between the predicted and experimental values of chip-tool interface temperature at different cutting conditions. Table 6 depicts the results predicted by the developed chip-tool interface temperature models for different tools. Predicted results can be seen in good agreement with the experimental results (Table 2) with an absolute error of less than 5%. However, the results predicted by the *ANN* model are shown with a better agreement with the experimental results as compared to statistical-based and dimensional analysis models.

It has been observed that the chip-tool interface temperature gets more affected with the cutting speed followed by the chip cross-sectional area and the specific cutting pressure. With the increase in the cutting speed, the requirement of the cutting energy increases resulting in high cutting temperature. The thermal conductivity of the cutting tool also has a major influence on the chip-tool interface temperature. Uncoated tool exhibited the lowest cutting temperature. This could be attributed to its higher thermal conductivity and large wear-out area of the tool during machining resulting in rapid dissipation of the interface heat into the tool.

A lower cutting temperature observed for single-layer *TiAlN* coated tool than multi-layer *TiN/TiAlN* coated tool, could be attributed to its higher thermal conductivity than the equivalent thermal conductivity of *TiN/TiAlN* coated tool. The lower thermal conductivity of the *TiN*/Ti*Al*N coated tool resists heat conduction resulting in more temperature on the rake face. This coated tool also exhibited higher cutting temperature than *AlTiCrN* and *AlTiN* coated inserts [21]. However, a higher cutting temperature with a multi-layer tool helps to make the material being machined relatively soft and therefore, can help in improving the machining performance. However, the lower cutting force was observed with the multi-layer *TiN/TiAlN*

coated carbide tool. This could be attributed to the lower coefficient of friction offered by the multi-layer tool rake surface to flowing chips as confirmed from the back surface of the chips. On the other hand, the highest cutting force was observed with uncoated carbide tools. The present study concludes that a comparative evaluation of the machining performance in terms of tool life, tool wear mechanisms, surface roughness, etc. is required while turning *SS304* using *PVD*-coated single later *TiAlN* and multi-layer *TiN/TiAlN* coated carbide tools.

Conclusions

Turning experiments on *SS304* austenitic stainless steel were performed with uncoated and PVD single-layer *TiAlN* and multi-layer *TiN/TiAlN* coated carbide tools. The classical tool-work thermocouple principle was used to measure the cutting temperature. The chip-tool interface temperature was investigated with statistical-based, dimensional analysis, and artificial neural network models. The following conclusions could be drawn.

• It was noticed that the chip-tool interface temperature depends more on the cutting speed followed by the chip cross-sectional area and the specific cutting pressure. Uncoated tool exhibited the lowest cutting temperature due to its higher thermal conductivity and large wear-out area of the tool during machining resulting in rapid dissipation of the interface heat into the tool.

• A lower cutting temperature was observed for the single-layer *TiAlN* coated tool than the multi-layer *TiN/TiAlN* coated tool. This could be attributed to its higher thermal conductivity than the equivalent thermal conductivity of the *TiN/TiAlN* coated tool. However, the lower cutting force was observed with the multi-layer *TiN/TiAlN* coated carbide tool that could be attributed to the lower coefficient of friction offered by the rake surface of this tool to flowing chips. On the other hand, the highest cutting force was observed with uncoated carbide tools.

• The results predicted by all the developed models for the temperature of the chip-tool interface for different tools are in good agreement with the experimental results with an absolute error of less than 5%. However, the results predicted by the *ANN* model showed better agreement with the experimental results than statistical-based and dimensional analysis models, and therefore, the developed *ANN* model can be reliably used for predicting chip-tool interface temperature during *SS304* turning.

References

1. Grzesik W. Experimental investigation of the cutting temperature when turning with coated indexable inserts. *International Journal of Machine Tools and Manufacture*, 1999, vol. 39, iss. 3, pp. 355–369. DOI: 10.1016/S0890-6955(98)00044-3.

2. Grzesik W. The role of coatings in controlling the cutting process when turning with coated indexable inserts. *Journal of Materials Processing Technology*, 1998, vol. 79, iss. 1–3, pp. 133–143. DOI: 10.1016/S0924-0136(97)00491-3.

3. Pal A., Choudhury S.K., Chinchanikar S. Machinability assessment through experimental investigation during hard and soft turning of hardened steel. *Procedia Materials Science*, 2014, vol. 6, pp. 80–91. DOI: 10.1016/j.mspro.2014.07.010.

4. Abhang L.B., Hameedullah M. Chip-tool interface temperature prediction model for turning process. *International Journal of Engineering Science and Technology*, 2010, vol. 2, iss. 4, pp. 382–393.

5. Alvelid B. Cutting temperature thermo-electrical measurements. *Annals of CIRP*, 1970, vol. 18, pp. 547–554.

6. Chinchanikar S., Choudhury S.K. Evaluation of chip-tool interface temperature: effect of tool coating and cutting parameters during turning hardened AISI 4340 steel. *Procedia Materials Science*, 2014, vol. 6, pp. 996–1005. DOI: 10.1016/j.mspro.2014.07.170.

7. Chinchanikar S., Choudhury S.K., Kulkarni A.P. Investigation of chip-tool interface temperature during turning of hardened AISI 4340 alloy steel using multi-layer coated carbide inserts. *Advanced Materials Research*, 2013, vol. 701, pp. 354–358. DOI: 10.4028/www.scientific.net/AMR.701.354.

8. Panneerselvam T., Kandavel T.K., Sreenivas S.A., Karthik S., Andru M.M. Effects of working parameters on performance characteristics of cutting tools processed through powder metallurgy under turning operation. *Journal of Materials Engineering and Performance*, 2021, vol. 30, iss. 4, pp. 2890–2898. DOI: 10.1007/s11665-021-05622-6.

9. Bapat P.S., Dhikale P.D., Shinde S.M., Kulkarni A.P., Chinchanikar S.S. A numerical model to obtain temperature distribution during hard turning of AISI 52100 steel. *Materials Today: Proceedings*, 2015, vol. 2, iss. 4–5, pp. 907–914. DOI: 10.1016/j.matpr.2015.07.150.

10. Dhar N.R., Ahmed M.T., Islam S. An experimental investigation on effect of minimum quantity lubrication in machining AISI 1040 steel. *International Journal of Machine Tools and Manufacture*, 2007, vol. 47, iss. 5, pp. 748–753. DOI: 10.1016/j.ijmachtools.2006.09.017.

11. Anagonye A.U., Stephenson D.A. Modeling cutting temperatures for turning inserts with various tool geometries and materials. *Journal of Manufacturing Science and Engineering*, 2002, vol. 124, iss. 3, pp. 544–552. DOI: 10.1115/1.1461838.

12. Kalss W., Reiter A., Derflinger V., Gey C., Endrino J.L. Modern coatings in high performance cutting applications. *International Journal of Refractory Metals and Hard Materials*, 2006, vol. 24, iss. 5, pp. 399–404. DOI: 10.1016/j.ijrmhm.2005.11.005.

13. Grzesik W., Nieslony P. Coupled thermo-mechanical FEM-based modelling of the tool-chip contact behaviour for coated cutting tools. *International Journal of Machining and Machinability of Materials*, 2012, vol. 11, iss. 1, pp. 20–35. DOI: 10.1504/IJMMM.2012.044920.

14. Jiang F., Yan L., Rong Y. Orthogonal cutting of hardened AISI D2 steel with TiAlN-coated inserts – simulations and experiments. *International Journal of Advanced Manufacturing Technology*, 2013, vol. 64, pp. 1555–1563. DOI: 10.1007/s00170-012-4122-3.

15. Grzesik W., Nieslony P. Prediction of friction and heat flow in machining incorporating thermophysical properties of the coating-chip interface. *Wear*, 2004, vol. 256, iss. 1–2, pp. 108–117. DOI: 10.1016/S0043-1648(03)00390-9.

16. Knight W.A., Boothroyd G. *Fundamentals of metal machining and machine tools*. CRC Press, 2005. 602 p. ISBN 9781138502246.

17. Whitney E.D. *Ceramic cutting tools: materials, development and performance*. William Andrew, 2012. 381 p. ISBN 9780815516316.

18. Drucker D.C., Ekstein H. A dimensional analysis of metal cutting. *Journal of Applied Physics*, 1950, vol. 21, no. 2, pp. 104–107. DOI: 10.1063/1.1699607.

19. Sekulic S. Investigation of tangential forces in metal cutting by dimensional analysis. *Periodica Polytechnica Mechanical Engineering*, 1976, vol. 20, no. 2, pp. 55–64.

20. Naderpour H., Kheyroddin A., Amiri G.G. Prediction of FRP-confined compressive strength of concrete using artificial neural networks. *Composite Structures*, 2010, vol. 92, no. 12, pp. 2817–2829. DOI: 10.1016/j.compstruct.2010.04.008.

21. Kulkarni A.P., Sargade V.G. Characterization and performance of AlTiN, AlTiCrN, TiN/TiAlN PVD coated carbide tools while turning SS 304. *Materials and Manufacturing Processes*, 2015, vol. 30, no. 6, pp. 748–755. DOI: 10.1080/10426914.2014.984217.

Conflicts of Interest

The authors declare no conflict of interest.